Original Research Article

Effect of Dosage and Seawater Mixing on the Hydration and Phase Evolution of OPC-CSA Paste

ABSTRACT

Using fiber-reinforced polymer as reinforcement has opened unprecedented opportunities for the use of seawater in concrete production, particularly in arid regions, island nations, and water-stressed communities, providing potential economic and environmental benefits. This study investigated the effect of CSA dosage and seawater mixing on the hydration kinetics, setting time, phase assemblage, and compressive strength development of binary ordinary Portland cement and calcium sulfoaluminate cement paste using complementary experimental techniques, including isothermal calorimetry, Vicat needle technique, X-ray diffraction, thermodynamic modeling, and compressive strength testing. Increased CSA dosage in a deionized water (DI) mixed system enhanced the heat of hydration, increased initial ettringite formation, and accelerated renewed aluminate reaction, resulting in faster setting time. However, the heat intensity of the main (alite) hydration period was reduced, resulting in slightly reduced early-age compressive strength. On the other hand, seawater mixing slightly reduced initial ettringite formation, shortened the dormant period and promoted alite reaction. Consequently, the initial setting time of plain 100% OPC system (M1) was reduced while that of OPC-CSA systems (M2 and M3) slightly increased. Seawater also reduced the dissolution of ye'elemite, increased and stabilized ettringite, and delayed monosulfate formation due to the preferred chloride binding by AFm phases, resulting in the preferred formation of Friedel's salt. Seawater mixing increased the early-age compressive strength of M1, M2, and M3 systems due to the promotion of alite reaction. However, the compressive strength reduced slightly at 28 days. The results of this study demonstrate the possibility of tailoring the early-age properties of OPC-CSA systems with seawater.

Keywords: Seawater, Hydration kinetics, Phase assemblage, Setting time, Calcium sulfoaluminate cement, Thermodynamic modeling, Compressive strength

1. INTRODUCTION

The use of fiber-reinforced polymer as reinforcement has renewed interest in seawater use for concrete production [4, 6, 7]. This approach is particularly beneficial to arid regions, water-stressed communities and island nations where freshwater sources face the adverse effect of climate-induced drought [1, 2, 3]. However, the elevated levels of chloride (Cl^-), sulfate (SO_4^{2-}), magnesium (Mg^{2+}), and sodium (Na^+) ions present in SW has been reported to significantly affect the hydration, microstructure and mechanical performance of cement-based materials [5, 6, 7, 8]. For instance, there is a consensus on hydration promotion leading to reduced setting time and enhanced early-age strength of ordinary Portland cement (OPC) by SW [6, 7, 8, 9]. Chloride ions in seawater accelerate the hydration of tricalcium silicate (C_3S) and dicalcium silicate (C_2S) due to increased ionic activity in the pore solution, leading to increased formation of calcium silicate hydrate (C-S-H) and portlandite (CH) [7]. However, the SW effect on the long-term strength of OPC-based concrete is still debatable, with some studies reporting reduced long-term strength [6, 8, 11, 12, 13, 15], while others claim increased long-term strength [13, 14, 16, 17]. While there may be some reduction in strength at later ages compared to freshwater mixing, as suggested in some

of the literature reviewed, the differences are not significant enough to preclude the use of SW in water-stressed environments [10]. While most studies found in the literature are primarily OPC-based systems, SW mixing of alternative cement, such as calcium sulfoaluminate cement (CSA), also garners interest. Jiang et al., 2024 [11] stated that SW has some effect on the hydration product of CSA cement, with ettringite and aluminum hydroxide being the main hydration products. They highlighted that more ettringite (Aft) is produced in freshwater (FW) compared to SW on the first day due to initial rapid ettringite precipitation on CSA particles in the SW system, preventing further hydration. The reduction in initial ettringite formed has been reported to extend the setting time and reduce mechanical strength in SW-mixed CSA cement [12]. Jiang et al., 2024 [11] revealed that SW mixing at normal concentrations (3.3%) enhanced compactness, thereby improving the strength and ductility of CSA-based mortar, while higher concentrations (6.6% and 9.9%) resulted in a slight decrease in its compressive strength. In addition, they highlighted the formation of Friedel's salt (FS) and the promotion of ettringite growth due to increased gypsum formed from the interaction between sulfate ions in SW and calcium ions from dissolved CSA clinker (see Equation 1). The formation of Friedel's and Kuzel's salts due to the chloride binding activity of aluminate ferrite monosubstituted (AFm) phases monocarbonate, hemicarbonate, and monosulfate (AFm-SO_4) has been reported elsewhere [11,16, 17], suggesting that chloride ions from SW are more competitive than sulfate ions at binding AFm phases (see Equation 2). Elsewhere, Wang et. al., 2024 [14] highlighted the impacts of different sea salt ions (sulfate, chloride, and magnesium) on the hydration properties and mechanical performance of a CSA system partially replaced with 10% OPC. Their findings revealed that Cl^- accelerated the hydration of CSA, sulfate ions elevated alkalinity and reduced mechanical strength, while magnesium ions diminished porosity and improved strength. The findings from previous studies suggest that the impact of seawater mixing on cement hydration kinetics can vary depending on the composition of seawater, cement type, and clinker composition [15].

$$SO_4^{2-} + Ca^{2+} + 2H_20 \rightarrow CaSO_4.2H_2O \quad (1)$$

$$3CaO.Al_2O_3.CaSO_4.12H_2O + 2Cl^- \rightarrow 3CaO.Al_2O_3.CaCl_2.10H_2O + SO_4^{2-} + 2H_2O \quad (2)$$

Meanwhile, the synergistic benefits of reduced carbon footprint, rapid setting, high early strength, shrinkage compensation, and enhanced sulfate and chloride resistance present OPC-CSA blends as a viable alternative binder for special applications such as rapid repairs and additive manufacturing of concrete [19, 22, 23, 24]. OPC's chemical composition and hydration process significantly differ from CSA in that CSA cements generally contain higher alumina, abundant sulfate, and lower calcium oxide and silica than OPC. The main clinker phases of CSA are ye'elemite ($C_4A_3\$$), belite (C_2S), and calcium sulfate (anhydrite), and its main hydration products are ettringite ($C_6A\$_3H_{32}$), amorphous aluminum hydroxide (AH_3) and monosulfate ($C_4A\$H_{12}$) [19]. On the other hand, the main hydration products of OPC are C-S-H and portlandite (CH) [20]. The hydration of freshwater-mixed OPC-CSA blends is well understood and can be summarized in Equations 3-6 [25, 26, 27, 28]. The setting of OPC-CSA blended systems is mainly facilitated by the hydration of ye'elemite and by the formation of ettringite (Equation 3), while the significant strength-giving phase is C-S-H that originates from the hydration of C_3S [21] (see Equation 5). Hence, CSA plays a vital role in setting and early-age mechanical properties, while OPC is mainly responsible for long-term mechanical and durability properties.

$$C_4A_3\$ + 2C\$ + 38H = C_6A\$_3H_{32} + 2AH_3 \quad (3)$$

$$C_4A_3\$ + 18H = C_4A\$H_{12} + 2AH_3 \quad (4)$$

$$C_3S + 3H = C - S - H + CH \quad (5)$$

$$6CH + 2AH_3 + 2C_6A\$_3H_{32} = 3C_4A\$H_{12} + 8H \quad (6)$$

One of the major challenges identified with OPC-CSA blends is the delay in alite hydration, which may compromise short-term and long-term mechanical and durability performance [30, 31, 32]. This delay has been attributed to several factors, such as rapid consumption of mix water by ettringite formation; coating of OPC particles by the ettringite formed, hindering water from reaching them for hydration; and the release of aluminum ions from ye'elemite dissolution [31, 32, 33]. While several hypotheses have been postulated to cause the delay in alite reaction with increased CSA dosage, the delay mechanism is not completely understood. Meanwhile, chloride ions present in SW have been reported to accelerate the hydration of OPC [7], while sulfate ions present in SW have been reported to delay the initial formation of ettringite while stabilizing its formation at later stages of hydration [12,18, 19, 20]. Against this backdrop, we hypothesize that seawater mixing will promote the reaction of alite in blended OPC-CSA systems, thereby improving its early-age and long-term mechanical properties. The extension of seawater mixing to blended OPC-CSA systems is incumbent upon a better understanding of its effect on the hydration process and the development of mechanical properties. To this end, this study aims to investigate the effect of seawater mixing on the hydration kinetics, phase assemblage, and evolution of early-age mechanical properties of blended OPC-CSA systems using complementary experimental techniques. Isothermal calorimetry is employed to monitor the heat of hydration at early ages, while quantitative XRD supported by thermodynamic simulations is used to determine the hydrated phase assemblage. The setting time is measured using the Vicat needle test, while the mechanical properties development is determined using the compressive strength testing method. We hope these research findings will provide helpful insight into extending the application of seawater mixing to blended OPC-CSA systems for the ecological and economic benefits of water-stressed communities and coastal regions.

2. MATERIAL AND METHODS

Commercially available Type I/II OPC and CSA cement with their crystalline clinker phase composition presented in Table 1 were employed as binders for this study. Sea salt from Lake Products Company was used to simulate seawater in compliance with ASTM D 1141-98. The chemical composition of the simulated seawater is presented in Table 2. The seawater mixtures were juxtaposed with deionized (DI) water-mixed systems, which served as a reference.

Table 1: Crystalline Clinker Phase Composition of CSA and OPC Cement

Crystalline Clinker Phase	CSA (%)	OPC (%)
Ye'elemite	40.6	-
β-Belite	24.4	13.1
Anhydrite	21.5	-
Alite	6.7	68.2
Ferrite	5.4	10.1
Aluminate	1.4	2.7
Gypsum	-	5.9

Table 2: Chemical Composition of Simulated Seawater

Chemical	Composition (g/l)
NaCl	24.53
$MgCl_2.6H_2O$	5.2
Na_2SO_4	4.09
$CaCl_2$	1.16
KCl	0.695
$NaHCO_3$	0.201
KBr	0.101
H_3BO_3	0.027
$SrC_{12}.6H_2O$	0.025
NaF	0.003

2.1 Sample Preparation

All materials used for this study were equilibrated at laboratory temperature for 24 hours before the start of all experiments. Six cement paste systems with mix design details presented in Table 3 were prepared and studied. All systems were mixed at a water-to-binder ratio of 0.35 and a curing temperature of 23°C. Anhydrous OPC and CSA were measured and blended to homogeneity using a Hamilton Beach electric mixer to prepare the paste. Afterward, mixing water was gradually added and mixed at speed 1 for 30 seconds, followed by speed 2 for 60 seconds. The paste was left for 30 seconds while cement stuck on the side of the mixing container was scrapped. The paste was finally mixed at speed 2 for 60 seconds. This procedure follows a recommendation similar to that of ASTM C305.

Table 3: Mix Design of Cement Paste Systems Investigated

Mix ID	OPC (%)	CSA (%)	Mix Water
M1 - DW	100	0	DI water
M1 - SW	100	0	Seawater
M2 – DW	80	20	DI water
M2 – SW	80	20	Seawater
M3 – DW	70	30	DI water
M3 – SW	70	30	Seawater

2.2 X-ray Diffraction Analysis

To determine the phase assemblage of hydrated cement systems, samples were taken from the same batches prepared for isothermal calorimetry and cast in a 20mm diameter plastic mold wrapped with parafilm.at desired ages (1 hour, 1 day, 7 days, and 28 days), 2 mm – 3 mm thick slices were cut from the hydrated paste and soaked in isopropanol for 20 minutes to stop hydration, followed by oven drying at 40°C for 15 minutes to remove the isopropanol. The slices were placed on Empyrean series two diffractometer (Figure 1a) with 2θ configuration and Cu Kα radiation (λ=1.54Å). Triplicate samples of each mix were scanned for 30 minutes each between 4° and 65°. Profex open-source software was used for phase identification and quantification via Rietveld analysis with a CoV of less than 3% [25]. All crystal structure files (except Friedel's salt and Kuzel's salt) used for Rietveld analysis were retrieved from the Bergmann and Kleeberg's Generalized Model for Neutron and X-ray diffraction (BGMN) repository integrated with Profex software [26]. The crystallographic information of Friedel's and Kuzel's salt was gotten from the Inorganic Crystal Structure Database (ICSD) and Crystallography Open Database (COD) databases, respectively [27].

2.3 Compressive Strength

The compressive strength evolution of DI water and seawater mixed systems was measured in compliance with ASTM C109 using the INSTRON universal testing machine (Figure 1b). Triplicate samples of each mix were prepared and cast in a 50 mm by 50 mm cubic mold and left to cure in the mold for 1 day before demolding and transferring them into a well-sealed plastic bag and left to cure in a humidity chamber at 23 °C until desired ages (1 hour, 1 day, 3 days, and 7 days) of testing. One hour and 1-day samples were tested immediately after removal from the molds, and the average of three tests was determined as the compressive strength for each mix.

2.4 Isothermal Calorimetry

An eight-channel TAM Air isothermal calorimeter (Figure 1c) was used to monitor the heat of hydration of hydrating systems at a curing temperature of 23°C. Portland cement was employed as a reference, and the specific heat capacities of binders were determined using the Hot Disk method according to ASTM C1113M-09. Triplicate samples of each mix were prepared as described previously and placed in the calorimeter with the reference material. Heat flow rate and cumulative heat released normalized by a unit gram of cement were acquired and analyzed (n = 3, coefficient of variance (CoV) < 3%).

2.5 Setting Time

Humboldt's VICATRONIC (Figure 1d) was employed to measure the time of setting of seawater-mixed and DI water-mixed systems according to ASTM C 191-21. Triplicate samples of each mix were prepared and poured into the Vicat molds, and the instrument's needle was programmed to penetrate the samples at 1-minute intervals for a total of 41 penetrations. The penetration resistance of the samples was plotted against time since contact with water. The initial setting time was calculated using Equation 6, while the final setting time was taken as the time to 40 mm (100%) penetration resistance. The setting time is reported in minutes to the nearest minute (n = 3, CoV < 5%).

$$\left(\left(\frac{H-E}{C-D}\right) * (C-25)\right) + E \quad (6)$$

Where E is the time in minutes of last penetration higher than 25 mm, H is the time in minutes of first penetration less than 25 mm, C is the penetration reading at time E, and D is the penetration reading at time H.

2.6 Thermodynamic Modeling

To better understand the mechanisms of hydration kinetics and hydrated phase formation, thermodynamic modeling based on Gibb's minimization energy technique was performed via GEM-Skeletor software coupled with the Cemdata18 database [28]. Thermodynamic modeling is a valuable tool for understanding the evolution of cement systems' hydration kinetics and microstructural properties. It is also essential for gaining further insight into the processes governing the dissolution and precipitation of hydrated phases. Rietveld analysis was performed to determine clinker dissolution kinetics for predicting hydrated phase assemblage, while the chemical composition of simulated seawater was employed to model the seawater-mixed system. Thermodynamic data for all aqueous species were obtained from the PSI-GEMS thermodynamic database, while the solubility products of cement minerals were retrieved from the Cemdata18 database [30, 31].

Fig 1. Instruments used for the experimental program: (a) Empyrean series 2 diffractometer used to acquire X-ray diffraction patterns of the hydrated specimen, (b) INSTRON universal testing machine, (c) TAM Air isothermal calorimeter used to monitor the heat of hydration, and (d) Humboldt's VICATRONICS used to measure setting time

3. RESULTS AND DISCUSSION

3.1 Heat of Hydration Kinetics

The results of heat flow rate and cumulative heat released measured by isothermal calorimetry provide a reliable indication of the hydration kinetics of cement systems. while the hydration of OPC systems is characterized by an initial heat of dissolution, a dormant period followed by the main heat peak corresponding to silicate reaction, then renewed aluminate reaction shoulder, and finally, steady, slow increase in the heat of hydration, the heat flow signature of OPC-CSA is uniquely different. Depending on the dosage of CSA, OPC-CSA heat flow kinetics comprise the initial heat due to the dissolution of reactive sulfates, partial dissolution of gypsum, aluminate, and initial ettringite precipitation [31]. This is followed by an intermediate peak corresponding to ettringite formation from the reaction of ye'elemite and calcium sulfate, the dormant period, and the heat flow peak attributed to the silicate reaction. The position of renewed aluminate is incumbent upon the degree of sulfate in the system. Highly sulfated systems usually have a renewed aluminate after the silicate peak, while under-sulfated systems have a renewed aluminate before the silicate peak.

3.1.1 Effect of CSA Dosage on the Heat of Hydration

The effect of CSA dosage on the heat of hydration of M1, M2, and M3 systems are presented in Figure 2a and 2b. Increased CSA dosage enhanced the initial heat of dissolution and the intermediate peak corresponding to ettringite formation. The increase in ettringite directly implies the increase in ye'elemite and calcium sulfate (gypsum and anhydrite) proportions. Compared to M1 - DW, increased CSA shortened the dormant period and accelerated the main heat peak corresponding to the silicate reaction while reducing its peak heat flow intensity in M2 - DW. On the other hand, the dormant period of M3 – DW was significantly extended up to 18 hours. The heat flow intensity of the silicate reaction was characteristically low and broadened, indicating a delayed reaction of alite at high CSA dosages. Previous studies have established the delayed reaction of alite in blended OPC-CSA systems incorporating high CSA proportion [30, 31, 32]. Meanwhile, the renewed aluminate peak was enhanced and accelerated with increased CSA dosage due to the rapid consumption of calcium sulfate by ye'elemite. For instance, the renewed aluminate shoulder reduced from 18 hours in the M1 – DW system to approximately 8 hours and 1.5 hours in the M2 – DW and M3 -DW systems, respectively. The cumulative heat released increased with CSA dosage up to 9 hours and subsequently dropped in M3 -DW system due to delayed alite reaction (see Fig. 2b). The cumulative heat released in M1 – DW, M2 – DW, and M3 -DW was approximately 175mW/g_{cement}, 190 mW/g_{cement} and 150mW/g_{cement} respectively.

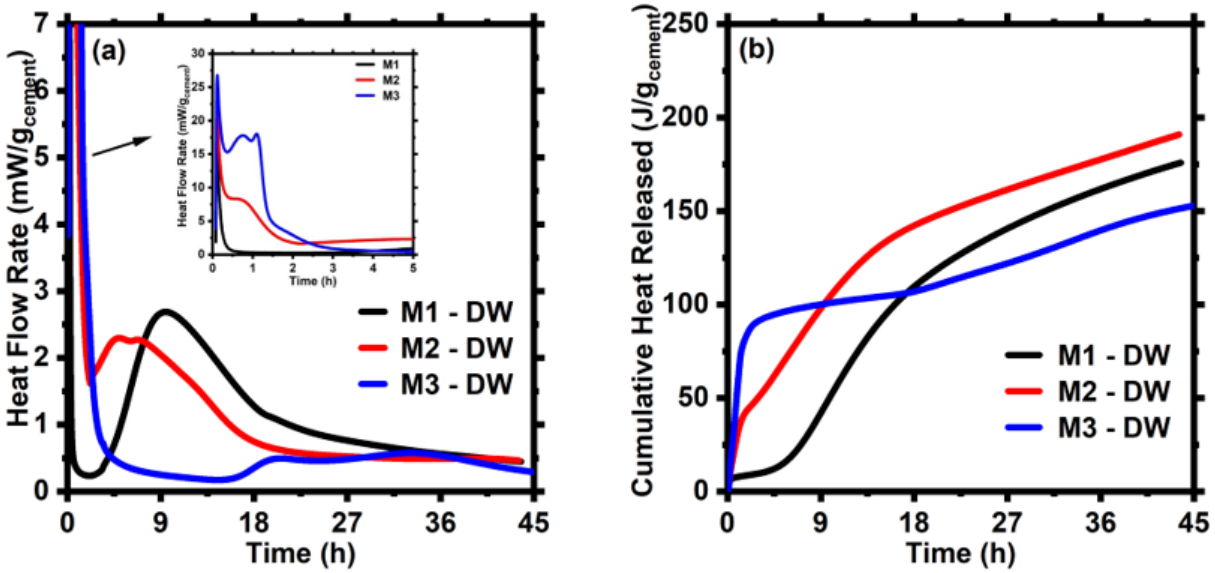

Fig 2. (a) The heat flow rate of M1 – DW, M2 – DW and M3 – DW and (b) the cumulative heat released in M1 – DW, M2 – DW and M3 – DW systems at 45 hours of hydration.

3.1.2 Effect of Seawater on the Heat of Hydration Kinetics

The effect of seawater on the heat flow rate and cumulative heat released by M1, M2, and M3 systems are shown in Figures 3 - 5. In the M1 system, seawater mixing shortened the induction period and accelerated the main heat peak associated with the silicate reaction. For instance, the heat flow rate at the main peak was increased by approximately 40%. The acceleration of alite reaction by chloride ions present in seawater has been reported in the literature [8, 9]. The renewed

aluminate peak was not obvious and may possibly have overlapped with the silicate peak. Seawater mixing also increased the cumulative heat released in M1 at 40 hours by approximately 5% (Figure 3b).

Seawater mixing slightly reduced the intermediate peak corresponding to ettringite formation in the M2 system. The initial rapid precipitation of ettringite on CSA cement particles inhibiting its further hydration has been suggested to reduce ettringite formation in seawater-mixed CSA cement in the first hour of hydration [11]. Similarly, the formation of gypsum from ionic activities between calcium and sulfate ions reduces the amount of sulfate ions available to react with ye'elemite in the first hour of hydration [34]. Increased gypsum in seawater-mixed systems is responsible for increased ettringite formation at later ages [20, 41]. Like the M1 system, seawater mixing slightly shortened the dormant period and accelerated the heat flow rate at the main peak associated with silicate reaction, indicating the promotion of alite reaction. This has implications for early-strength development in OPC-CSA systems. However, renewed aluminate shoulder was slightly delayed in M2 – SW due to the increased formation of gypsum from ionic activities of seawater [33].The cumulative heat released in the first 40 hours of hydration was not significantly affected by seawater mixing of the M2 system (Figure 4b).

Similar to the M2 system, seawater mixing slightly reduced the intermediate peak corresponding to ettringite formation in the M3 system while enhancing the heat flow at the main peak, indicating the promotion of alite reaction (Figure 5a). Compared to M3 – DW, the induction period of M3 – SW was shortened by approximately 16 hours, while the heat flow rate at the main heat peak was enhanced by 360%. This result shows the potential of seawater to improve the early-age strength of OPC-CSA incorporating a high dosage of CSA. The renewed aluminate peak of M3 – SW was not obvious; it may have overlapped with the main heat peak. Seawater mixing increased the cumulative heat released in the M3 system at 60 hours by approximately 12.5%.

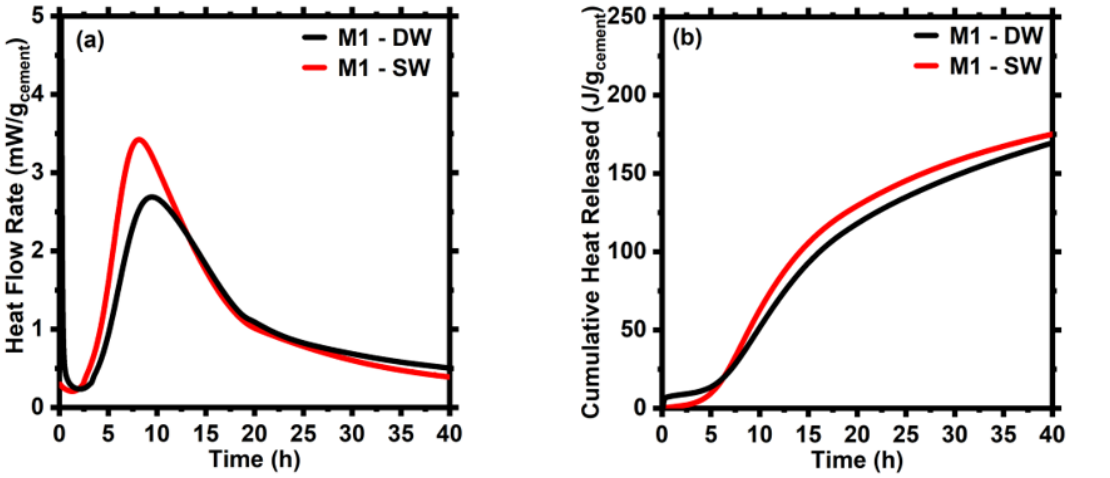

Fig 3. (a) Heat flow rate (b) cumulative heat released for M1-DW and M1-SW at 40 hours from mixing

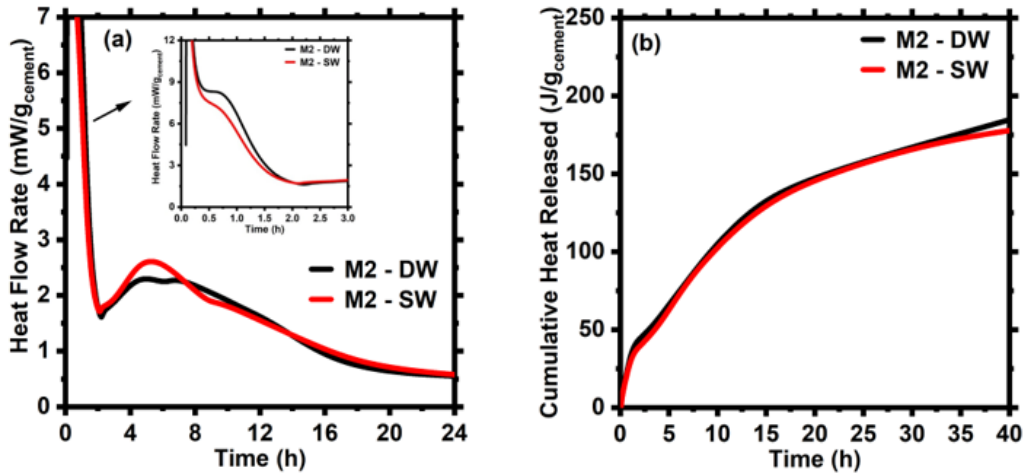

Fig 4. (a) heat flow rate at 24 hours, and (c) cumulative heat released at 40 hours for M3-DW and M3-SW

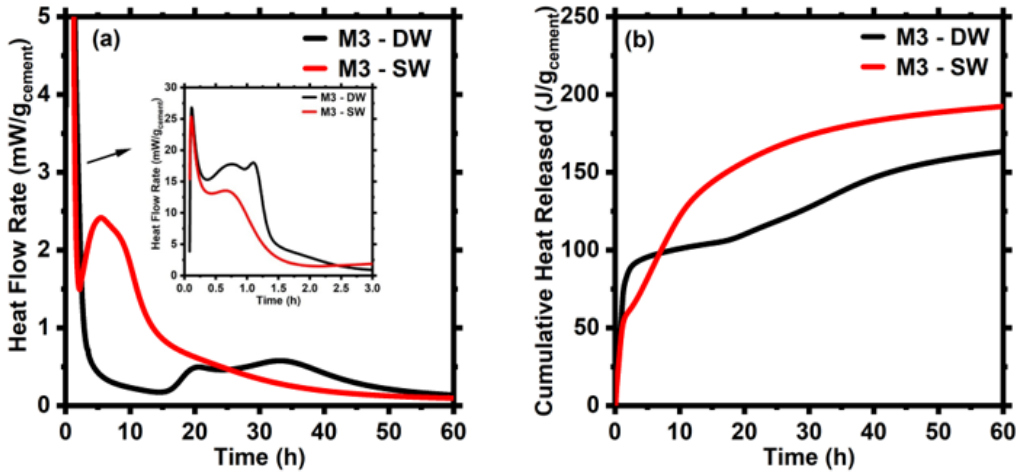

Fig 5. (a) Heat flow rate at 60 hours, and (b) cumulative heat released at 60 hours for M4-DW and M4-SW.

3.2 Setting Time

Representative curves of penetration resistance and the initial setting times measured by the Vicat needle technique are presented in Figures 6a and 6b, respectively. Increased CSA dosage accelerated the time to penetration resistance and the initial setting time due to the rapid ettringite formation from the reaction of ye'elemite and calcium sulfate. CSA is mainly responsible for OPC-CSA systems' fast setting and high early strength. For instance, the initial setting time was reduced from 246 minutes in M1 – DW to 21.29 minutes and 16.5 minutes in M2 – DW and M3 – DW systems, respectively. The reduced initial setting time supports the enhanced intermediate peak corresponding to ettringite formation in isothermal calorimetry results (Figure 2a). Seawater mixing reduced the initial setting time of the M1 system by 19.4%. This result supports the enhanced main heat peak observed in isothermal calorimetry (Figure 3a). The acceleration of OPC hydration due to increased ionic activities in seawater has been reported in previous studies [8, 9, 10]. Contrarily, the initial setting time of M2 and M3 systems were delayed by 16.8% and 24.8%, respectively, due to the reduced formation of ettringite in the first hour of hydration, corroborating the reduced intermediate peaks observed in Figures 4a and 5a. Increased sulfate ions present in seawater favor the initial formation of gypsum by reacting with dissolved calcium in the pore solution [21, 34]. This claim is supported by the XRD results presented in a later section.

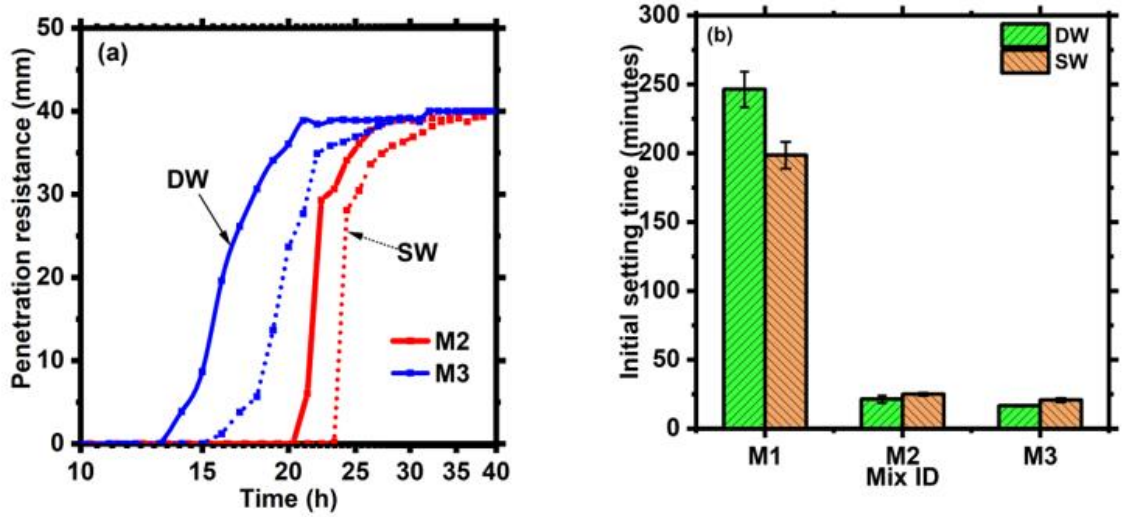

Fig 6. (a) Representative penetration resistance curves of M2, M3, and M4 and (b) Average initial setting time of M1, M2, M3, and M4 systems. (n = 3, CoV < 5%). Note: The bold lines represent DW-mixed systems, while the dotted lines represent SW-mixed systems

3.3 Phase Assemblage

3.3.1 Effect of CSA Dosage on Phase Assemblage

The effect of CSA dosage on the early-age hydration and phase formation of OPC-CSA is shown in Figures 7a and 7b. At 6 hours, increased CSA dosage enhanced ettringite's peak intensity at 9.2° 2θ. This confirms the enhanced initial heat release observed in isothermal calorimetry. On the other hand, portlandite peak intensity located at 18.2° 2θ reduced with increased CSA dosage, indicating reduced silicate reaction and C-S-H formation. This confirms the reduced heat flow intensity of the silicate peak observed in isothermal calorimetry. While gypsum was observed at 10.8° 2θ in the M1 – DW system at 6 hours, it was completely reacted in the M2 – DW and M3 – DW systems, supporting the accelerated appearance of renewed aluminate peak seen in isothermal calorimetry results. Further, the peak intensity associated with alite and belite increased with increased CSA dosage, confirming the reduction of the degree of reaction. A similar observation was seen at 1 day of hydration except for the complete gypsum reaction in the M1 – DW system and the appearance of monosulfate peak at 11.23 in the M2 – DW system. The ettringite peak was slightly enhanced, while the aluminate peak was not seen in M2 – DW and M3 – DW systems, indicating its complete reaction. At 28 days of hydration, ye'elemite had completely reacted in M2 – DW and M3 – DW, resulting in enhanced ettringite and the appearance of monosulfate peaks. The monosulfate peak of M1 – DW is not obvious due to its poor crystallinity. The complete reaction of aluminate was also observed in all systems studied. Portlandite peak was reduced while alite and belite peaks increased with CSA dosage, indicating reduced C-S-H formation. This may have implications for mechanical performance, as seen in a later section.

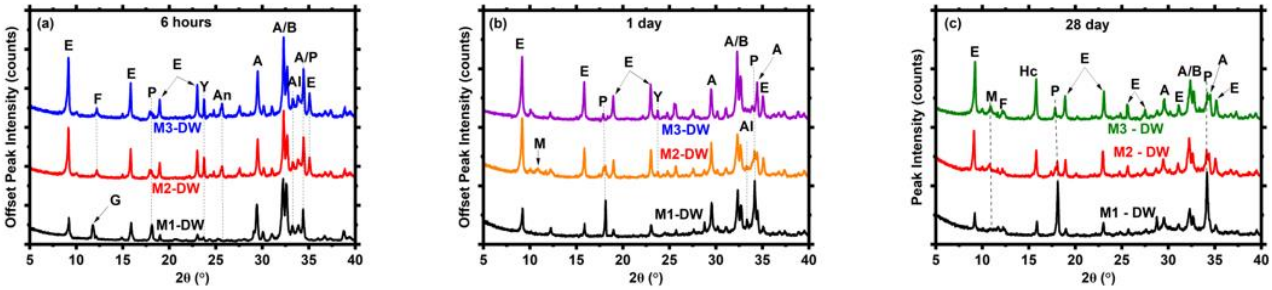

Fig 7. X-ray diffraction pattern of M1 -DW, M2 – DW and M3 – DW at (a) 6 hours and (b) 1 day (c) 28 days of hydration. A – alite, Al – aluminate, B – belite, E - ettringite, F – ferrite, G – gypsum, M -monosulfate, P -portlandite, Y – ye'elemite

3.3.2 Effect of Seawater Mixing on Phase Assemblage

The diffraction patterns of deionized-mixed and seawater-mixed M1 systems were compared in Figure 8. Starting with the M1 (plain 100% OPC) system, at 6 hours of hydration, seawater mixing reduced ettringite peak indicating reduced ye'elemite reaction. This observation supports the reduced intermediate heat flow peak intensity in Figures 4a and 5a. A similar observation of reduced ettringite formation in SW was also reported in the first hours of hydration [11]. Similarly, the gypsum peak was enhanced in the M1 – SW system due to its increased early formation in seawater systems. Increased gypsum formation in seawater due to the reaction of Na_2SO_4 with calcium ion species, thereby reducing the SO_4 ions in pore solution, has been reported by [34]. The reduced ettringite peak intensity seen at 6 hours in M1 – SW can also be attributed to reduced SO_4 in the pore solution. Meanwhile, portlandite peak intensity was enhanced while alite/belite peak were slightly reduced compared to M1 – DW, indicating accelerated alite reaction. This result supports the enhanced silicate peak seen in Figure 3a. The acceleration of alite's reaction due to increased ionic activities in seawater systems has been widely published in the literature [6, 7, 8, 9]. Aluminate peak was also seen in M1 – DW and M1 – SW systems. At 1 day of hydration of M1 systems, gypsum had completely depleted in M1 – DW and M1 – SW systems, confirming the renewed aluminate peaks observed at around 18 hours in Figure 3a. The Ettringite peak was enhanced in M2 – SW, indicating increased C-S-H formation in seawater system. At 28 days, the ettringite peak was enhanced in M1 – SW while it was reduced in M1 – DW system due to its conversion to monosulfate. This observation confirms the stability of ettringite in seawater-mixed cement systems. Jiang, et. al., 2024 [11] recently reported the stability of ettringite in seawater-mixed systems. Monosulfate was seen in M1 – DW at 10.8° 2θ, while Friedel's salt was observed in M1 – SW at 11.2° 2θ due to the chloride binding activity of monosulfate. It has been suggested that chloride ions from seawater are more competitive than sulfate ions at binding AFm phases [11,16]. Further, aluminate was completely reacted in both M1 – DW and M1 -SW systems, while alite/belite peaks were reduced in the M1 – DW system, indicating their increased reaction degree at later ages.

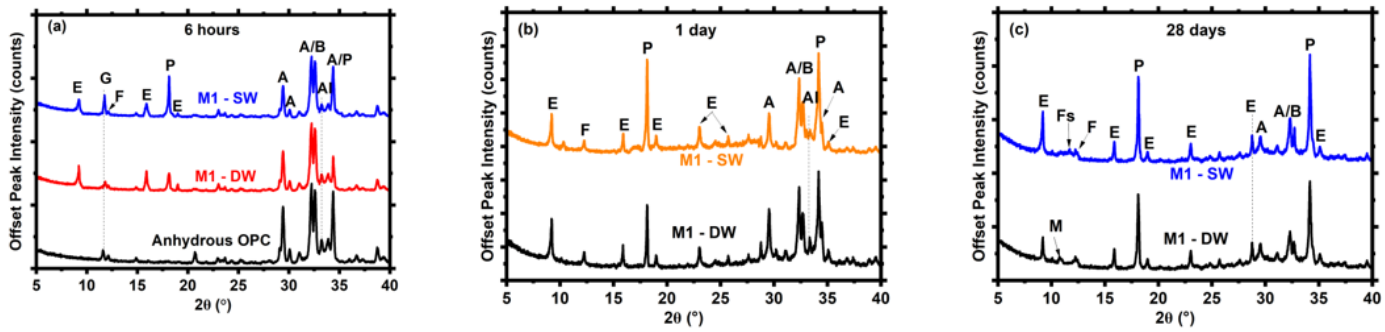

Fig 8. The diffraction patterns of M1 – DW and M1 – SW at (a) 6 hours, (b) 1 day (c) 28 days. A – alite, Al – aluminate, B – belite, E - ettringite, F – ferrite, Fs – Friedel's salt, G – gypsum, M -monosulfate, P -portlandite.

Figures 9a, 9b, and 9c show the effect of seawater mixing on M2 systems at 6 hours, 1 day, and 28 days of hydration. At 6 hours, seawater mixing reduced ettringite peak intensity due to the rapid initial precipitation of ettringite on CSA particles, inhibiting its further hydration [11]. Similarly, the ye'elemite peak was enhanced in M2 – SW, indicating its slower reaction in seawater. This may be due to the initial rapid ettringite precipitation on CSA particles hindering its further hydration. Portlandite peak was enhanced in M2 – SW, confirming the acceleration of alite's reaction and increased C-S-H formation at early ages. Meanwhile, the anhydrite peak was enhanced in the M2 – SW system. This may explain the slight delay in the appearance of the renewed aluminate peak shown in isothermal calorimetry results (Figure 4a). The aluminate peak was also slightly enhanced in the M2 – SW system, indicating its delayed dissolution in seawater systems. At 1 day, ettringite peak intensity was enhanced in M2 – SW while aluminate was completely reacted in both M2 – DW and M2 – SW systems. Anhydrite also persisted in both M2 – DW and M2 – SW systems, while the peak intensity of ye'elemite increased in the M2 – SW system, indicating its reduced dissolution in seawater. Portlandite peak reduced in both systems possibly due to its reaction with ettringite and gibbsite to form monosulfate according to Equation 6. Meanwhile, monosulfate peak was not observed in the X-ray diffraction pattern, maybe present in amorphous form. Increased alite and belite peaks in M2- SW indicate its reduced reaction degree. At 28 days, ettringite peak remained stable in M2 – SW while it reduced in M2 – DW system. monosulfate was observed in M2 – DW system while both monosulfate and Friedel's salt overlap in M2 – SW system. While portlandite peak was enhanced in M2 – SW system, alite and belite peaks intensities increased compared to M2 – DW system. This observation suggests that increased portlandite peak may not necessarily indicate increased C-S-H formation. Increased ionic activities between calcium and hydroxide may have resulted in increased portlandite formation in seawater. While ye'elemite had completely reacted in M2 – DW system, its diffraction peak was still prominent in M2 – SW system.

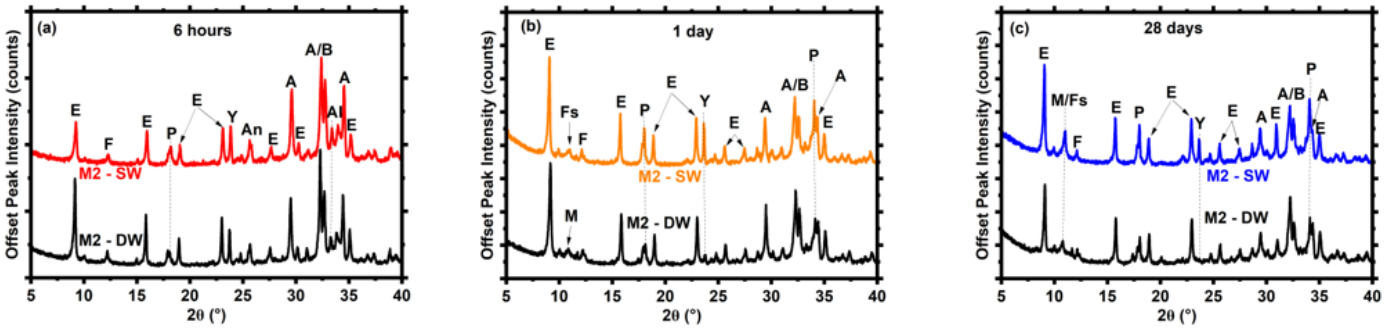

Fig 9. The diffraction patterns of M2 – DW and M2 – SW at (a) 6 hours, (b) 1 day (c) 28 days. A – alite, Al – aluminate, B – belite, E - ettringite, F – ferrite, Fs – Friedel's salt, G – gypsum, M -monosulfate, P -portlandite, Y – ye'elemite

The diffraction patterns of M3 – DW and M3 – SW systems at 6 hours, 1 day, and 28 days are presented in Figures 10a, 10b, and 10c, respectively. The effect of seawater on the M3 system is similar to the results of the M2 system except for increased ettringite peak, reduced portlandite peak, and reduced alite and belite dissolution. Of note is the significant delay in alite dissolution confirmed by the enhanced diffraction peak intensity at 1 day in the M3 – DW system. This result supports the extended dormant period observed in isothermal calorimetry (Figure 5a). However, the dissolution of alite/belite increased in the M3 – DW system at 28 days, as shown by its reduced diffraction peak intensity (Figure 10c).

In summary, seawater mixing reduced ettringite formation in the first hours of hydration but later increased its stability in later ages. Alite's reaction was also accelerated by seawater mixing, while renewed aluminate was slightly delayed in M2 and M3 systems. The dissolution of ye'elemite and anhydrite was delayed while gypsum's formation increased in seawater systems.

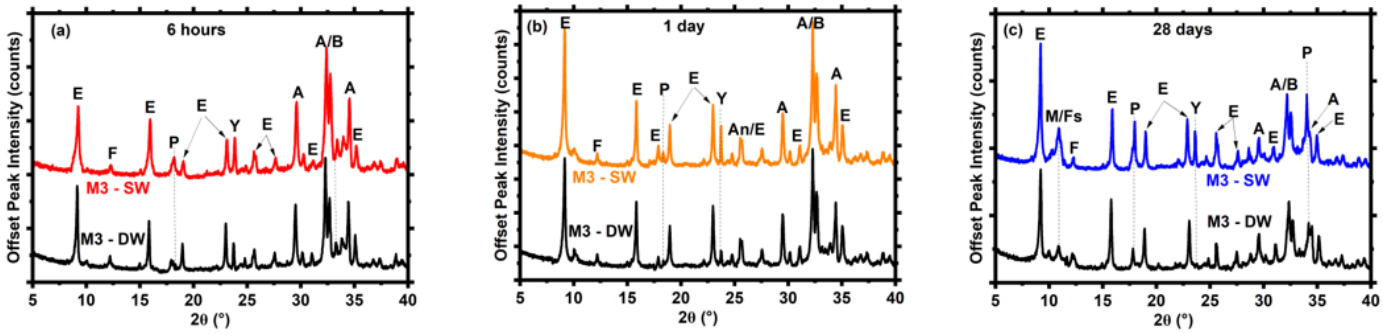

Fig 10. The diffraction patterns of M3 – DW and M3 – SW at (a) 6 hours, (b) 1 day (c) 28 days. A – alite, Al – aluminate, B – belite, E - ettringite, F – ferrite, Fs – Friedel's salt, G – gypsum, M -monosulfate, P -portlandite, Y – ye'elemite.

3.3.3 Predicted Phase Assemblage

Thermodynamic modeling of cement paste is useful for understanding the effect of cement composition and other effects on phase changes and chemical interactions that occur during the hydration of cement clinkers. To support the observations from isothermal calorimetry and X-ray diffraction, thermodynamic modeling was performed on the six systems studied, and the results are presented in Fig. 11 a-f. Increased CSA dosage accelerated and increased the volume of ettringite and AFm phases (monosulfate and Friedel's salt) formed in M2 and M3 systems while reducing the volumes of portlandite and C-S-H. This result supports the observations in isothermal calorimetry and X-ray diffraction. Further, increased CSA accelerated the consumption of gypsum due to its early reaction with ye'elemite to form ettringite supporting the accelerated appearance of renewed aluminate peak observed in isothermal calorimetry (Figure 2a) and the absence of gypsum diffraction peak in M2- DW and M3 – DW at 6 hours (Figure 7a). Overall, the initial hydrated phase volume increased with CSA dosage because of the rapid formation of ettringite. This has implications for early strength development in OPC-CSA systems.

The effect of seawater mixing on the phase assemblage of M1 systems includes increased ettringite volume, formation of Friedel's salt instead of monosulfate, and increased early C-S-H and portlandite formation. The slow dissolution of ye'elemite in seawater may have contributed to the continuous formation of ettringite in M2 – SW and M3 – SW systems. The dissolution of alite was also accelerated in the first hours by seawater missing (see figures 10a and 10b). In the M2 system comprising 80% OPC and 20% CSA, seawater mixing reduced the initial ettringite formed, reduced and delayed monosulfate formation due to preferred chloride binding of AFm phases leading to Friedel's salt formation. Further, seawater mixing increased ettringite volume at later ages, supporting the enhanced ettringite diffraction peak intensities observed in XRD results (Figure 9c). Seawater also increased initial C-S-H and portlandite in M2 – SW and M3 – SW systems corroborating the enhanced portlandite peaks observed in XRD results (Figure 9 and 10). Seawater mixing also increased initial gypsum formed in M2 – SW and M3 – SW systems. Seawater mixing also reduced the initial hydrated phase volume in M2 – SW and M3 – SW due to reduced early ettringite formation.

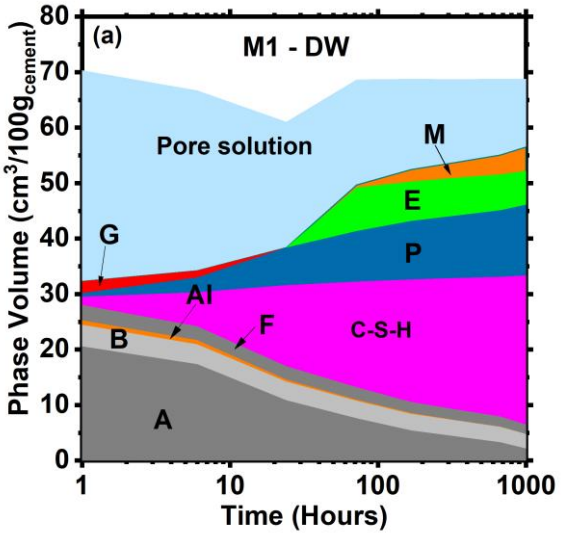
(a)
M1 - DW
Pore solution
M
E
G
P
Al
F
C-S-H
B
A
Phase Volume (cm3/100gcement)
Time (Hours)

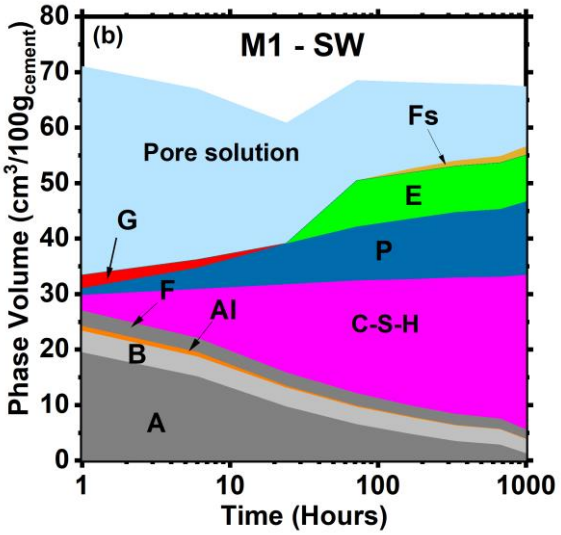
(b)
M1 - SW
Pore solution
Fs
E
G
P
F
Al
C-S-H
B
A
Phase Volume (cm3/100gcement)
Time (Hours)

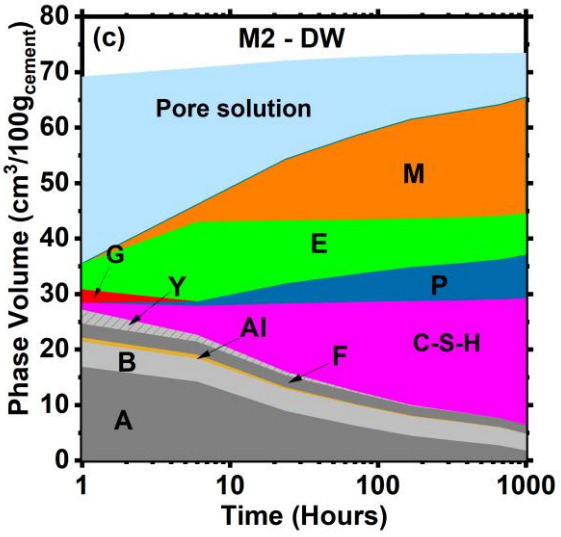
(c)
M2 - DW
Pore solution
M
G
E
Y
P
Al
C-S-H
F
B
A
Phase Volume (cm3/100gcement)
Time (Hours)

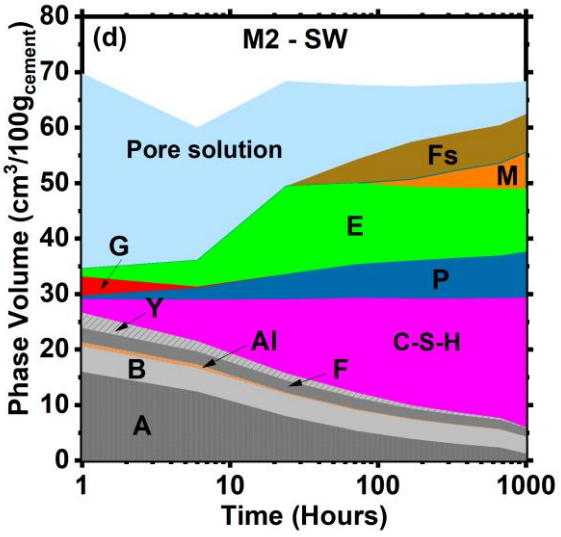
(d)
M2 - SW
Pore solution
Fs
M
G
E
P
Y
Al
C-S-H
F
B
A
Phase Volume (cm3/100gcement)
Time (Hours)

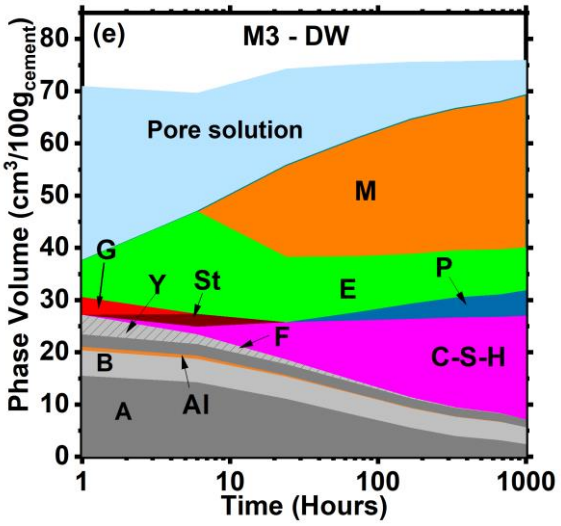
(e)
M3 - DW
Pore solution
M
G
Y
St
E
P
F
C-S-H
B
A
Al
Phase Volume (cm3/100gcement)
Time (Hours)

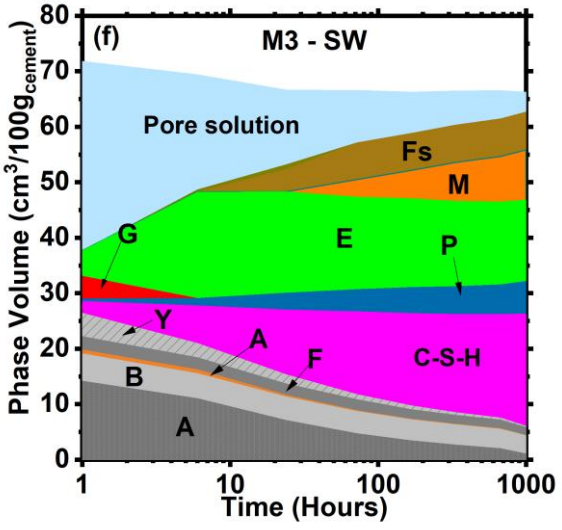
(f)
M3 - SW
Pore solution
Fs
M
G
E
P
Y
A
F
C-S-H
B
A
Phase Volume (cm3/100gcement)
Time (Hours)

Fig 11. Predicted Phase Assemblage of (a) M3-DW, (b) M3-SW, (c) M4-DW, and (d) M4-SW via GEMS thermodynamic simulation.

3.4 Compressive Strength

The average compressive strength evolution of M1, M2, and M3 systems are presented in Figures 9 a-d. Increased CSA dosage accelerated the average compressive strength at 0.04 days due to the rapid ettringite precipitation in the first hour of hydration. This result is corroborated by the enhanced ettringite diffraction peak intensities observed at 6 hours in M2 – DW and M3 – DW (Figure 7a). On one day, the compressive strength of D1 – DW was 23.56 MPa, while those of M2 – DW and M3 – DW were 33.67 MPa and 21.86 MPa, respectively, supporting the cumulative heat-released results in isothermal calorimetry results (Figure 2b). At 28 days, increased CSA dosage slightly reduced the compressive strength of M2 – DW and M3 – DW by approximately 2.17% and 6.46%, respectively. The 28 days compressive strength results agree with the reduced portlandite peak and increased alite/belite peaks shown in XRD results (Figure 7c) and reduced C-S-H volume thermodynamically predicted with increased CSA dosage in figures 11 a, c, and e). C-S-H is mainly responsible for the long-term strength of OPC-CSA systems [21] hence, there is a slight reduction in compressive strength with increased CSA dosage. The compressive strength of M3 – DW also evolved slowly at 1 day due to the delayed hydration of alite, confirming the extended dormant period observed in the isothermal calorimetry result (Figure 2a).

Seawater mixing increased the compressive strength of the M1 system up to 3 days and slightly reduced the same by approximately 2.2% at 28 days. The promotion of early hydration of alite by seawater has been reported in the literature [6, 10, 17]. Contrarily, seawater mixing slightly reduced the compressive strength of the M2 system at 0.04 and 1 day while slightly increasing the same at 3 and 28 days. This slight reduction in early-age strength agrees with the reduction in hydrated phase volume predicted by thermodynamic simulation (Figures 11c and 11d). The effect of seawater mixing on the early-age compressive strength of M3 was significant. Notably, seawater mixing reduced the compressive strength of M3 by 16.79% at 0.04 days while increasing the same by 54.38% and 9.12% at 1 and 3 days, respectively. However, the strength of the M3 system was reduced by 1.2% at 28 days. The significant increase in compressive strength seen at 1 day is due to the promotion of alite reaction agreeing with isothermal calorimetry, XRD, and thermodynamic simulations.

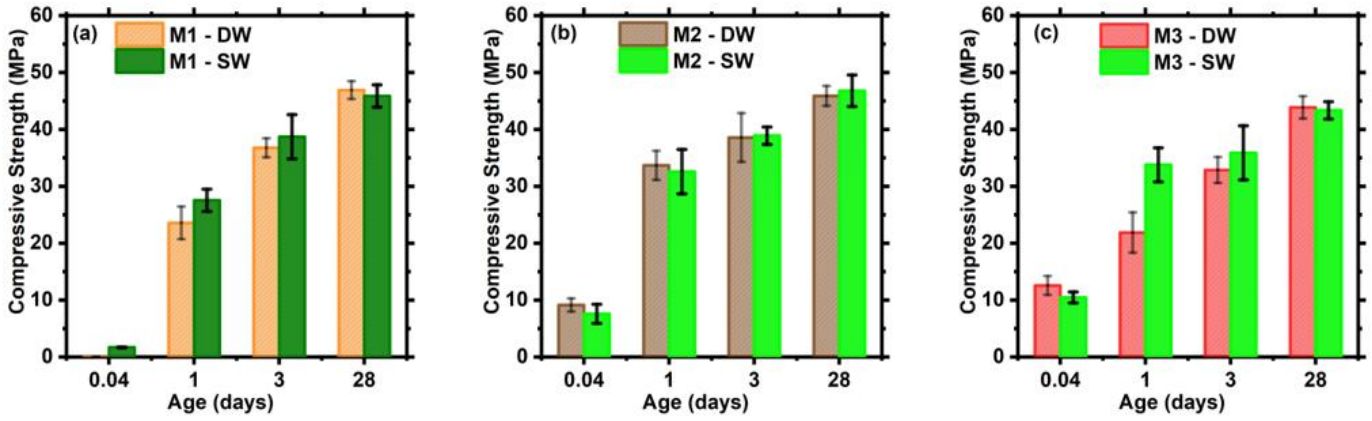

Fig 12. The average compressive strength evolution of (a) M1-DW and M1-SW, (b) M2-DW and M2-SW, (c) M3-DW and M3-SW at 0.04 days, 1 day, 3 days, and 28 days (n = 3, coefficient of variance < 5%)

4. Discussion

The isothermal calorimetry analyses highlight the complex interplay between CSA dosage, seawater mixing, and hydration kinetics in OPC-CSA blended cement systems. Notably, the influence of CSA dosage on hydration behavior is significant, as it modifies the sequence and intensity of key hydration events, including the silicate and aluminate reactions. The findings demonstrate that higher CSA dosages lead to increased initial heat of dissolution and ettringite formation. However, delayed alite hydration at elevated CSA levels, as observed in the M3-DW system, reflects a trade-off between rapid initial reactions and more extended induction periods. The acceleration of the aluminate reaction with higher CSA dosage underscores the importance of optimizing sulfate availability. Insufficient sulfate in high-CSA systems exacerbates aluminate reactions, shifting peak times and potentially affecting early-age microstructure development. While the cumulative heat released in the M1 and M2 systems generally increased with CSA dosage, the reduction in cumulative heat for M3-DW highlights the inhibitory effect of delayed alite hydration. This aligns with prior studies suggesting limited alite reactions in highly sulfated systems.

The influence of seawater as a mixing medium further emphasizes the sensitivity of OPC-CSA systems to ionic environments. Chloride ions in seawater accelerated the silicate reaction across all mixes, resulting in higher heat flow rates

at the main hydration peak. This effect is particularly pronounced in the M3 system, where seawater mixing shortened the dormant period by 16 hours and significantly enhanced the heat flow intensity, suggesting improved early-age strength potential. The formation of gypsum through ionic interactions in seawater-mixed systems appears to have reduced early ettringite formation, but this effect diminishes with increasing hydration time. A notable observation is the absence or overlap of the renewed aluminate peak in seawater-mixed systems, particularly at higher CSA dosages. This behavior might be attributed to the accelerated consumption of sulfate ions and the potential interference of chloride ions with ettringite stability. The 12.5% increase in cumulative heat for the M3-SW system over the M3-DW system at 60 hours reinforces the hypothesis that seawater enhances early-age hydration, albeit with varying effects depending on CSA dosage.

Overall, these results provide critical insights into the design of OPC-CSA blended systems for marine applications. By balancing CSA dosage and leveraging seawater's ionic contributions, tailored hydration profiles can be optimized for early-age strength and long-term durability. Further investigations into the microstructural evolution of these systems under varying sulfate and chloride conditions would provide additional clarity on the mechanisms driving these hydration behaviors.

The phase assemblage of OPC-CSA systems, as influenced by CSA dosage and seawater mixing, reveals critical insights into hydration kinetics and the development of cementitious phases. Increased CSA dosage significantly accelerated early-age hydration, marked by enhanced ettringite formation due to the rapid reaction of ye'elemite with sulfate ions. This was evident from the intensified ettringite peak at 9.2° 2θ at 6 hours, corroborating the calorimetric data indicating enhanced initial heat release. However, this acceleration was accompanied by a reduction in the reaction of silicate phases, as demonstrated by diminished portlandite and C-S-H formation, suggesting a trade-off between early-age reactivity and silicate hydration. By 28 days, the complete reaction of ye'elemite in higher CSA systems (M2 and M3) led to stabilized ettringite and the formation of monosulfate. However, reduced silicate reaction may have implications for long-term mechanical performance.

Seawater mixing introduced a distinct chemical environment influencing phase stability and reaction kinetics. In the early stages, seawater reduced ettringite formation due to limited sulfate availability in the pore solution, as observed in the diminished ettringite peak at 6 hours. This reduction was offset by the formation of gypsum and accelerated alite hydration, evidenced by increased portlandite and C-S-H formation. At later stages, seawater enhanced the stability of ettringite, delaying its conversion to monosulfate, particularly in systems with lower CSA content (M1). Furthermore, the formation of Friedel's salt in seawater systems, replacing monosulfate, underscores the competitive binding of chloride ions, which aligns with thermodynamic predictions and enhances the chloride resistance of these systems.

Thermodynamic modeling supported these experimental findings, showing increased ettringite and AFm phase volumes with CSA dosage alongside reduced portlandite and C-S-H volumes. In seawater systems, the delayed dissolution of ye'elemite and anhydrite sustained ettringite formation at later ages, while enhanced ionic activities accelerated alite hydration and portlandite formation in the early stages. These interactions suggest that seawater mixing can stabilize ettringite and promote chloride binding, potentially improving the durability of seawater-mixed systems under aggressive environments.

These results highlight the dual effects of CSA dosage and seawater mixing on the hydration process, with implications for both early-age performance and long-term durability. While increased CSA dosage promotes rapid early strength, it may compromise silicate hydration and long-term mechanical properties. Conversely, seawater mixing enhances the stability of ettringite and chloride binding, offering potential advantages for marine and chloride-rich environments. These findings provide a foundation for optimizing OPC-CSA formulations to balance early strength development and durability under varied environmental conditions.

5. Conclusions

This study elucidated the effect of CSA dosage and seawater mixing on the hydration kinetics, setting time, phase assemblage, and compressive strength evolution of blended OPC-CSA systems. The significant findings are summarized as follows:

- CSA dosage enhanced the initial heat of dissolution, the intermediate peak corresponding to ettringite formation, and shortened the dormant period. On the other hand, the heat flow intensity of the silicate peak was reduced, indicating a reduced reaction degree. The renewed aluminate peak and cumulative heat released were enhanced with increased CSA dosage. On the other hand, seawater mixing enhanced the initial heat of dissolution, shortened the dormant period and accelerated the silicate reaction. Contrarily, the intermediate peak associated with ettringite formation was slightly reduced, and the renewed aluminate peak was slightly delayed in seawater-mixed systems.
- Increased CSA significantly reduced the setting time of M1 – DW, M2 – DW and M3 – DW systems due to the rapid formation of ettringite. Similarly, seawater reduced the initial setting time of the M1 system while slightly increasing those of the M2 – SW and M3 – SW systems due to the reduced formation of ettringite in the first hour of hydration.
- In terms of phase assemblage, the same type of phases was predicted in all systems studied except for the appearance of strätlingite (which later converts to monosulfate) in the M3 – DW system in the early hours of hydration due to the delayed alite reaction. Increased CSA dosage enhanced ettringite formation at early ages of hydration and monosulfate at later ages, while C-S-H and portlandite formation reduced in M2 – DW and M3 – DW systems due to reduced alite reaction. Seawater mixing slightly reduced early ettringite formation, delayed ye'elemite dissolution and promoted the early formation of C-S-H and portlandite.

- Monosulfate was delayed and reduced in seawater systems due to the competitive binding of chloride to AFm phases forming Friedel's salt. The delayed formation of monosulfate resulted in increased and stabilized ettringite.
- The early-age compressive strength of CSA-dosed systems increased at early ages due to increased ettringite formation, while its 28-day strength was slightly reduced due to reduced C-S-H formation. Seawater mixing improved the early-age compressive strength of all systems studied due to its promotion of alite reaction. However, the 28-day compressive strength was slightly reduced in the M1 – SW and M3 – SW systems.

While this study presents some helpful insight into the effect of seawater mixing on the early-age properties of binary OPC-CSA systems, further research is needed to unravel the hydration mechanisms of ye'elemite in seawater systems. This way, the early ettringite formation and the later age reaction of ye'elemite can be optimized for improved performance. More so, the effect of seawater mixing on the structure and morphology of the hydrated phases formed would be worthy of research to pursue in the future.

Data Availability

The experimental data used to analyze the results is available upon reasonable request.

REFERENCES

[1] H. Varshney, R. A. Khan, and I. K. Khan, "Sustainable use of different wastewater in concrete construction: A review," *J. Build. Eng.*, vol. 41, p. 102411, Sep. 2021, doi: 10.1016/j.jobe.2021.102411.

[2] Y. Gwon, D. Kim, H. Lee, M. H. Yoo, S. H. Choi, and J. Park, "Method for Calculating Potential Direct Loss of Water Shortages by Water Use Type and Deducing Optimal Applications," 2024, doi: 10.5194/egusphere-egu24-5016.

[3] X. Li and J. Peng, "Joint effects of storage-runoff limitation amplify global stress in water availability," 2024, doi: 10.5194/egusphere-egu24-5652.

[4] H. Ritchie and M. Roser, "Water Use and Stress," *Our World Data*, Feb. 2024, Accessed: Aug. 13, 2024. [Online]. Available: https://ourworldindata.org/water-use-stress

[5] A. V. Savenko and V. S. Savenko, "On the Transformation of the Chemical Composition of Seawater in Interaction with Terrigenous Aerosols," *Oceanology*, 2020, doi: 10.1134/S0001437020050215.

[6] W. Lun Lam, P. Shen, Y. Cai, Y. Sun, Y. Zhang, and C. Sun Poon, "Effects of seawater on UHPC: Macro and microstructure properties," *Constr. Build. Mater.*, vol. 340, p. 127767, Jul. 2022, doi: 10.1016/j.conbuildmat.2022.127767.

[7] T. Lv, J. Zhang, L. Xu, D. Hou, W.-J. Long, and B. Dong, "Hydration behavior and chloride binding of seawater-mixed sintered sludge cement paste: Experimental and thermodynamic study," *Constr. Build. Mater.*, vol. 426, p. 136170, May 2024, doi: 10.1016/j.conbuildmat.2024.136170.

[8] F. M. Wegian, "Effect of seawater for mixing and curing on structural concrete," *IES J. Part Civ. Struct. Eng.*, vol. 3, no. 4, pp. 235–243, Nov. 2010, doi: 10.1080/19373260.2010.521048.

[9] N. Otsuki, H. Hamada, N. Takeda, T. Yamaji, T. Habuchi, and T. Nishida, "Technical Committee on the use of sea water in concrete," 2014.

[10] J. Xiao, C. Qiang, A. Nanni, and K. Zhang, "Use of sea-sand and seawater in concrete construction: Current status and future opportunities," *Constr. Build. Mater.*, vol. 155, pp. 1101–1111, Nov. 2017, doi: 10.1016/j.conbuildmat.2017.08.130.

[11] Z. Jiang, Z. Zhu, F. Accornero, and C. Wang, "Multi-technique analysis of seawater impact on the performance of calcium sulphoaluminate cement mortar," *Constr. Build. Mater.*, vol. 443, p. 137717, Sep. 2024, doi: 10.1016/j.conbuildmat.2024.137717.

[12] C. Wang, Z. Liu, T. Zhang, Y. Zhang, Z. Liu, and X. Zhao, "Influence of the Concentration of Seawater on the Early Hydration Properties of Calcium Sulphoaluminate (CSA) Cement: A Preliminary Study," *Buildings*, vol. 11, no. 6, Art. no. 6, Jun. 2021, doi: 10.3390/buildings11060243.

[13] M. D. A. Thomas, R. D. Hooton, A. Scott, and H. Zibara, "The effect of supplementary cementitious materials on chloride binding in hardened cement paste," *Cem. Concr. Res.*, vol. 42, no. 1, pp. 1–7, Jan. 2012, doi: 10.1016/j.cemconres.2011.01.001.

[14] C. Wang, S. Zhou, Q. Ou, and Y. Zhang, "Investigation on the Impacts of Three Sea Salt Ions on the Performance of CSA-OPC Binary System," *Buildings*, vol. 14, no. 5, Art. no. 5, May 2024, doi: 10.3390/buildings14051481.

[15] J. Wang *et al.*, "Effect of Phaeodactylum Tricornutum in Seawater on the Hydration of Blended Cement Pastes," *Coatings*, 2022, doi: 10.3390/coatings12111639.

[16] K. B. Hee, K. Y. Goo, K. K. Hoon, and C. J. Won, "OPC CSA Eco-friendly low-active CSA-based cement to replace ordinary portland cementOPC," 2018

[17] S. Park, N. Lee, and K.-G. Park, “Early-age hydration behavior of calcium sulfoaluminate (CSA) cement/ordinary Portland cement-blended ultra-high performance concrete,” *J. Build. Eng.*, vol. 87, p. 109058, Jun. 2024, doi: 10.1016/j.jobe.2024.109058.
[18] Z. Yang, H. Ye, Q. Yuan, B. Li, Y. Li, and D. Zhou, “Factors Influencing the Hydration, Dimensional Stability, and Strength Development of the OPC-CSA-Anhydrite Ternary System,” *Materials*, vol. 14, no. 22, Art. no. 22, Jan. 2021, doi: 10.3390/ma14227001.
[19] F. Winnefeld and B. Lothenbach, “Hydration of calcium sulfoaluminate cements — Experimental findings and thermodynamic modelling,” *Cem. Concr. Res.*, vol. 40, no. 8, pp. 1239–1247, Aug. 2010, doi: 10.1016/j.cemconres.2009.08.014.
[20] D. Jansen, F. Goetz-Neunhoeffer, B. Lothenbach, and J. Neubauer, “The early hydration of Ordinary Portland Cement (OPC): An approach comparing measured heat flow with calculated heat flow from QXRD,” *Cem. Concr. Res.*, vol. 42, no. 1, pp. 134–138, Jan. 2012, doi: 10.1016/j.cemconres.2011.09.001.
[21] L. Pelletier, F. Winnefeld, and B. Lothenbach, “The ternary system Portland cement–calcium sulphoaluminate clinker–anhydrite: Hydration mechanism and mortar properties,” *Cem. Concr. Compos.*, vol. 32, no. 7, pp. 497–507, Aug. 2010, doi: 10.1016/j.cemconcomp.2010.03.010.
[22] A. Kothari, I. Tole, H. Hedlund, T. Ellison, and A. Cwirzen, “Partial replacement of OPC with CSA cements – effects on hydration, fresh and hardened properties,” *Adv. Cem. Res.*, vol. 35, no. 5, pp. 207–224, May 2023, doi: 10.1680/jadcr.22.00054.
[23] S. Park, Y. Jeong, J. Moon, and N. Lee, “Hydration characteristics of calcium sulfoaluminate (CSA) cement/portland cement blended pastes,” *J. Build. Eng.*, vol. 34, p. 101880, Feb. 2021, doi: 10.1016/j.jobe.2020.101880.
[24] E. Rozière, A. Loukili, R. El Hachem, and F. Grondin, “Durability of concrete exposed to leaching and external sulphate attacks,” *Cem. Concr. Res.*, vol. 39, no. 12, pp. 1188–1198, Dec. 2009, doi: 10.1016/j.cemconres.2009.07.021.
[25] N. Doebelin and R. Kleeberg, “Profex: a graphical user interface for the Rietveld refinement program BGMN,” *J. Appl. Crystallogr.*, vol. 48, no. 5, pp. 1573–1580, Oct. 2015, doi: 10.1107/S1600576715014685.
[26] J. Bergmann, P. Friedel, and R. Kleeberg, “BGMN—a new fundamental parameters based Rietveld program for laboratory X-ray sources, its use in quantitative analysis and structure investigations,” *CPD Newsl.*, vol. 20, no. 5, pp. 5–8, 1998.
[27] A. Terzis, S. Filippakis, H.-J. Kuzel, and H. Burzlaff, “The crystal structure of Ca2Al(OH)6Cl · 2H2O,” *Z. Für Krist. - Cryst. Mater.*, vol. 181, no. 1–4, pp. 29–34, Dec. 1987, doi: 10.1524/zkri.1987.181.14.29.
[28] T. Wagner, D. Kulik, F. Hingerl, and S. Dmytrieva, “GEM-Selektor Geochemical Modeling Package: TSolMod Library and Data Interface for Multicomponent Phase Models,” *Can. Mineral.*, vol. 50, pp. 1173–1195, Dec. 2012, doi: 10.3749/canmin.50.5.1173.
[29] B. Lothenbach and F. Winnefeld, “Thermodynamic modelling of the hydration of Portland cement,” *Cem. Concr. Res.*, vol. 36, no. 2, pp. 209–226, Feb. 2006, doi: 10.1016/j.cemconres.2005.03.001.
[30] T. Matschei, B. Lothenbach, and F. P. Glasser, “The AFm phase in Portland cement,” *Cem. Concr. Res.*, vol. 37, no. 2, pp. 118–130, Feb. 2007, doi: 10.1016/j.cemconres.2006.10.010.
[31] K.-G. Park, “1. Early-age hydration behavior of calcium sulfoaluminate (CSA) cement/ordinary Portland cement-blended ultra-high performance concrete,” *J. Build. Eng.*, 2024, doi: 10.1016/j.jobe.2024.109058.
[32] G. Le Saoût, B. Lothenbach, A. Hori, T. Higuchi, and F. Winnefeld, “Hydration of Portland cement with additions of calcium sulfoaluminates,” *Cem. Concr. Res.*, vol. 43, pp. 81–94, Jan. 2013, doi: 10.1016/j.cemconres.2012.10.011.
[33] A. Younis, U. Ebead, P. Suraneni, and A. Nanni, “Fresh and hardened properties of seawater-mixed concrete,” *Constr. Build. Mater.*, vol. 190, pp. 276–286, Nov. 2018, doi: 10.1016/j.conbuildmat.2018.09.126.
[34] Y. Sun *et al.*, “Mechanisms on Accelerating Hydration of Alite Mixed with Inorganic Salts in Seawater and Characteristics of Hydration Products,” *ACS Sustain. Chem. Eng.*, vol. 9, no. 31, pp. 10479–10490, Aug. 2021, doi: 10.1021/acssuschemeng.1c01730.
[35] C. Shi, J. Yin, and C. Hu, “Microstructure, Hydration, and Chloride Binding Behavior of Limestone Calcined Clay Cement Prepared Using Seawater,” *J. Mater. Civ. Eng.*, 2023, doi: 10.1061/jmcee7.mteng-15838.